

A NONPARAMETRIC TECHNIQUE FOR HIGH PRECISION ESTIMATION OF POWER SYSTEM TIME-VARYING PHASORS

Rastko Zivanovic
Technikon Pretoria, South Africa

Abstract – In this paper, we present a non-parametric technique for estimation of time-varying phasors and frequency in power systems. In this approach, instantaneous RMS value and phase angle of either voltage or current phasor are obtained using Park transform followed by demodulation. A linear function is used to approximate these signals locally on the sliding window of variable length. Optimal window length is selected for each signal sample: large window if the signal is slow time-varying to improve filtering of noise and harmonics, and small window for sudden changes to make signal tracking more accurate. In order to make high precision estimates an approach that combines left-sided, central and right-sided windows is proposed in the paper. The paper concludes with the presentation of the examples based on simulated signals as well as real-life signals recorded during power swing condition in ESKOM transmission system.

Keywords: *Phasor measurement, Digital protection and control, Digital signal processing, Nonparametric statistics*

1 INTRODUCTION

An important component of the modern technology for power system protection and control is the estimation of the magnitude, phase and frequency content of voltage and current waveforms as they vary over time. Efforts to estimate these values are complicated by the presence of noise and interference in the recorded waveforms. This interference may be in the form of harmonics of the system fundamental frequency, or of interharmonics, which can be generated by periodically time-varying loads, or by circuits with multiple switching functions (such as FACTS devices). Traditional approach is to utilise the Parameter Estimation algorithm [1] that unifies a number of algorithms including the Discrete Fourier Transform. Unfortunately, these parametric algorithms could not adapt to changing system conditions. They could be designed either to accurately track magnitude, phase and frequency in the non-stationary and transient situations with the poor filtering of noise and interference, or with good filtering of the stationary waveforms but large bias in tracking system changes.

As an alternative to non-adaptive parametric class of algorithms, one could try to estimate time-varying phasors non-parametrically without reference to a specific signal model and with use of variable window size, as we demonstrated previously for the instantaneous frequency estimation [2]. The main goal of this paper is to present the application of the local linear modelling method for high precision estimation of the positive sequence time-varying phasors. This method has been

derived using Local Polynomial Approximation methodology [3]. Samples of the instantaneous RMS value or magnitude, and phase angle are obtained from three-phase waveforms by using Park transform and demodulation [4]. These samples are fitted locally on a sliding window with adaptive length. The local model is the first order Taylor polynomial. In the case of left-sided window, a window length is used to calculate the estimate for a single right endpoint q . When a new sample is available, the calculation repeats for the time point $q+1$ with different window length. For each time point the window length is selected to fulfil optimal criterion: balance of the estimator bias and variance. To estimate bias the significant derivatives must be known. These values are normally not available and therefore we use the algorithms that do not require bias to determine the optimal window and polynomial order [5,6]. It should be emphasised that the estimate is not assumed to be a polynomial function of time. This is the principal difference between the nonparametric approach and the parametric estimators [1]. To make the algorithm even more accurate the optimal estimates could be calculated for left, central and right window. By combining these results the final high precision result is obtained.

The paper concludes with the presentation of the representative simulation results as well as the results obtained in using ESKOM's Digital Fault Recorder (DFR) records. The results show that the algorithm is very accurate in estimating phasors and frequency for non-stationary and transient waveforms, and in presence of noise and interference.

2 THE PROPOSED TECHNIQUE

2.1 Time-varying Phasor

Root Mean Square (RMS) value and phase angle of either voltage or current complex phasor are calculated using Park transform [4]. If we consider three-phase voltage set $(v_a(q), v_b(q), v_c(q))$, result of the transformation are orthogonal components $v_d(q)$ and $v_q(q)$:

$$\begin{bmatrix} v_d(q) \\ v_q(q) \end{bmatrix} = \sqrt{\frac{2}{3}} \begin{bmatrix} 1 & -1/2 & -1/2 \\ 0 & \sqrt{3}/2 & -\sqrt{3}/2 \end{bmatrix} \begin{bmatrix} v_a(q) \\ v_b(q) \\ v_c(q) \end{bmatrix}. \quad (1)$$

The complex voltage signal $v_d(q) + jv_q(q)$ could be represented as the sum of time-varying harmonics:

$$v_d(q) + jv_q(q) = \sqrt{3} \sum_{k \geq 0} v_k(q) e^{jqk\theta_0}, \quad (2)$$

where $\theta_0 = \omega_0 T_s$ is the sampling angle (digital frequency), T_s is the sampling interval, and $\omega_0 = 2\pi f_0$ is the nominal fundamental frequency. Further on, the com-

plex voltage signal is shifted down (demodulated) in frequency domain to the angle value that corresponds to the nominal fundamental frequency:

$$\begin{aligned} \underline{v}_m(q) &= \frac{1}{\sqrt{3}}(v_d(q) + jv_q(q))e^{-jq\theta_0} \\ &= \underline{v}_1(q) + \sum_{k \geq 0, k \neq 1} \underline{v}_k(q)e^{jq(k-1)\theta_0}. \end{aligned} \quad (3)$$

Finally, the time-varying RMS value and phase angle of the complex phasor $\underline{v}_m(q) = v_m(q)\exp(j\varphi_m(q))$ are:

$$v_m(q) = \frac{1}{\sqrt{3}} \left| (v_d(q) + jv_q(q))e^{-jq\theta_0} \right|, \quad (4)$$

$$\varphi_m(q) = \arg \left(\frac{1}{\sqrt{3}}(v_d(q) + jv_q(q))e^{-jq\theta_0} \right). \quad (5)$$

It should be noted that the voltage phasor (3) comprises of the slow time-varying component (positive sequence) $\underline{v}_1(q)$, and the rest are fast time-varying oscillatory signals. If we consider linear network, response to some disturbance will consist of fundamental frequency signal plus transient component. Modes of the transient component could have frequency larger than fundamental mode. The resulting signal will have distorted sinusoidal shape. These modes are modelled in (3) as fast components. Signal distortions due to non-linear network components are typically represented as harmonics in (2), or as fast components in (3). For the frequencies of the transient modes smaller than fundamental frequency the resulting signal is modulated sinusoid. These types of modes are represented in (3) with the slow time-varying component. We can also expect fundamental frequency variation after large disturbances. This variation belongs to the slow time-varying component in the model (3). The main goal of the non-parametric approximation of $v_m(q)$ and $\varphi_m(q)$ is to filter out fast components in (3) and noise, and at the same time, to achieve maximum accuracy in tracking variations of the positive sequence phasor $\underline{v}_1(q)$.

2.2 The Non-parametric Approximation

In this approach we approximate time-varying RMS value (4) and phase angle (5) with a local linear model. The coefficients of the model are estimates of the value itself and the first derivative. The approximation is valid locally, on a left-sided sliding data window with variable length, and it is obtained through fitting samples to a linear model by minimizing the least squares objective functions:

$$\frac{1}{n+1} \sum_{k=0}^n [v_m(q-k) - v(q) + v'(q)kT_s]^2, \quad (6)$$

$$\frac{1}{n+1} \sum_{k=0}^n [\varphi_m(q-k) - \varphi(q) + \omega(q)kT_s]^2. \quad (7)$$

By solving the least squares problems (6) and (7) the expressions for the coefficients estimates (RMS, angle and frequency) are obtained in the filter form:

$$\hat{v}(q) = \sum_{k=0}^n h_v(k, n) v_m(q-k), \quad (8)$$

$$\hat{\varphi}(q) = \sum_{k=0}^n h_\varphi(k, n) \varphi_m(q-k), \quad (9)$$

$$\hat{\omega}(q) = \frac{1}{T_s} \sum_{k=0}^n h_\omega(k, n) \varphi_m(q-k), \quad (10)$$

where the weight sequences are calculated using:

$$h_v(k, n) = h_\varphi(k, n) = \frac{1}{n+1} \left(1 + 3 \frac{n-2k}{n+2} \right), \quad (11)$$

$$h_\omega(k, n) = \frac{6(2k-n)}{n(n+1)(n+2)}. \quad (12)$$

Hence, the instantaneous frequency estimator at the sample q is given by

$$\hat{f}(q) = f_0 + \frac{\hat{\omega}(q)}{2\pi}. \quad (13)$$

2.3 Accuracy as the Function of Window Length

The main idea of the proposed technique is to vary the window length with each new sample; i.e. to use long window for steady state or slow-varying signal and short window for fast-varying signal. Long data window will efficiently filter out fast varying oscillatory components and noise, while a short window will reduce bias in tracking signal variations. It is clear that the central issue in the window length selection is the compromise between filtering and tracking performance. Therefore, it is crucial to analyse the bias and variance of the filters (8), (9) and (10) as a function of window length.

The RMS voltage and phase angle can be modelled using non-linear function plus modelling error ε . It is assumed that the modelling errors belong to the class of independently and identically distributed random numbers with zero mean and variances σ_v^2 and σ_φ^2 . The non-linear functions are approximated on the time points $(q-k)T_s$ that are comprising the left-sided window. The second order Taylor series is used in these approximations

$$v_m(q-k) \approx v(q) - v'(q)kT_s + v''(q)(kT_s)^2/2 + \varepsilon, \quad (14)$$

$$\varphi_m(q-k) \approx \varphi(q) - \omega(q)kT_s + \omega'(q)(kT_s)^2/2 + \varepsilon. \quad (15)$$

The following expressions for bias and standard deviation estimates are calculated by using approximations (14) and (15) for v_m and φ_m in the filter expressions (8), (9), and (10):

$$\hat{b}_v(q, n) = \frac{\text{bias}}{12f_s^2} v''(q), \quad \hat{\sigma}_v(n) = \frac{\text{standard deviation}}{\sqrt{(n+1)(n+2)}} \sigma_v, \quad (16)$$

$$\hat{b}_\varphi(q, n) = \frac{n(n-1)}{12f_s^2} \varphi''(q), \quad \hat{\sigma}_\varphi(n) = \frac{\sqrt{2(2n+1)}}{\sqrt{(n+1)(n+2)}} \sigma_\varphi, \quad (17)$$

$$\hat{b}_\omega(q, n) = \frac{n}{2f_s} \omega'(q), \quad \hat{\sigma}_\omega(n) = \sqrt{\frac{12}{n(n+1)(n+2)}} f_s \sigma_\phi, \quad (18)$$

where $f_s = 1/T_s$ is the sampling frequency.

The standard deviations σ_v and σ_ϕ can be estimated in the robust way using Median Absolute Deviation (MAD) estimator $\text{median}(|d|)/(0.6745\sqrt{2})$, where each entry of the vector d is calculated as the difference between two consecutive samples of either v_m or ϕ_m .

According to (16), (17) or (18), bias is a deterministic error completely defined by the rate of change of underlining signal at the point qT_s , window length and sampling frequency. The sampling frequency should be constant which makes practical implementation easier, while window length will vary to control the bias in tracking RMS value, angle or frequency. The standard deviations in (16), (17), and (18) are representing the stochastic errors determined by the standard deviations σ_v and σ_ϕ , window length and sampling frequency. For a constant sampling frequency, the varying window length controls the standard deviation of the estimates. The standard deviation reduction factors $\sqrt{2(2n+1)/(n+1)(n+2)}$, $\sqrt{12/(n(n+1)(n+2))}$ in (16), (17) and (18) are decreasing functions of window length n as shown in Figure 1.

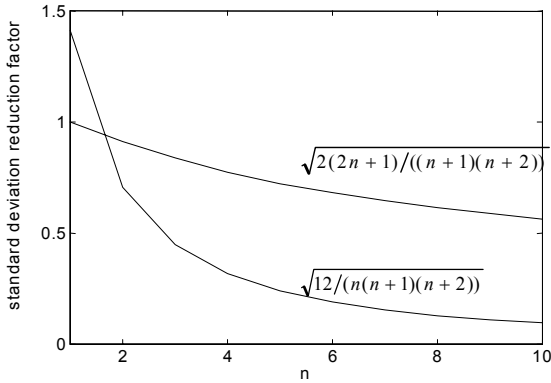


Figure 1: Standard deviation reduction factors in function of window length

Mean Square Error (MSE) criterion could be used to estimate local accuracy of the filters (8), (9) and (10). The local MSE criterion combines bias and standard deviation in the following expression:

$$\hat{J}(q, n) = \text{bias}(q, n)^2 + s.\text{deviation}(n)^2, \quad (19)$$

where bias and $s.\text{deviation}$ are defined according to (16), (17) and (18). The straightforward way of determining the optimal window length by solving $\partial\hat{J}(q, n)/\partial n = 0$ is not possible in practice because the rate of change ($v''(q)$ or $\omega'(q)$) is not known in advance.

2.4 Window Selection Algorithm

For slow variation of the signal, a large window should be used to filter out noise and fast oscillatory

components in (3), and if the signal changes are fast, a small window must be used to reduce the bias in signal tracking. Therefore, a reasonable choice of the window to be used is the one that balances bias and variance.

To find the optimal window length one needs to calculate estimates (RMS value, angle or frequency) for several different window lengths. Then each candidate estimate should be assessed to select the best one. The assessment is based on the Intersection of Confidence Intervals method (ICI) [5,6]. In this method, after calculating the estimates $\hat{v}(q)$, $\hat{\phi}(q)$ and $\hat{\omega}(q)$ using (8), (9) and (10) respectively, for window length $n+1$, the corresponding confidence intervals have to be estimated as follows:

$$\hat{D}_v(q, n) = [\hat{v}(q) - \kappa\hat{\sigma}_v(n), \hat{v}(q) + \kappa\hat{\sigma}_v(n)], \quad (20)$$

$$\hat{D}_\phi(q, n) = [\hat{\phi}(q) - \kappa\hat{\sigma}_\phi(n), \hat{\phi}(q) + \kappa\hat{\sigma}_\phi(n)], \quad (21)$$

$$\hat{D}_\omega(q, n) = [\hat{\omega}(q) - \kappa\hat{\sigma}_\omega(n), \hat{\omega}(q) + \kappa\hat{\sigma}_\omega(n)], \quad (22)$$

where $\hat{\sigma}_v(n)$, $\hat{\sigma}_\phi(n)$, and $\hat{\sigma}_\omega(n)$ are calculated using the expressions (16), (17) and (18), and κ is a threshold of confidence interval. For each new sample q , the estimates $\hat{v}(q)$, $\hat{\phi}(q)$ and $\hat{\omega}(q)$, and the corresponding confidence intervals (20), (21) and (22), for the specified window lengths are calculated. If we use 5 dyadic window lengths (6, 12, 24, 48, and 96), 5 estimates and 5 confidence intervals will be calculated for each value (RMS value, angle, or frequency). To illustrate the idea of ICI method we are using frequency estimation as an example. When a generator frequency is steady, the MSE is dominated by the stochastic error. By increasing the window length the standard deviation of this error and MSE will reduce, as shown in Figure 2. The largest window (96 samples) provides the most accurate result. Since, the signal is steady, the bias stays zero for all window lengths. In this example frequency is 55Hz and the standard deviation of the phase angle samples is 0.6%.

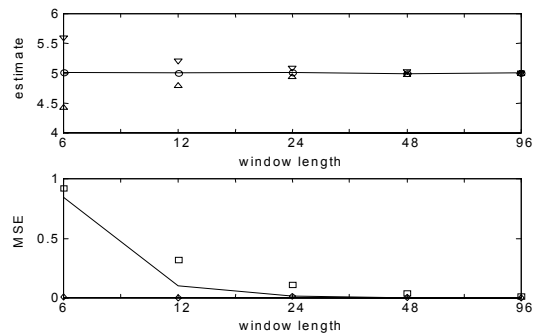


Figure 2: The steady-state frequency case: Estimates of $\hat{\omega}(q)/2\pi$ (circles), common points of confidence intervals $\hat{D}_\omega(q, n)/2\pi$ (triangles), standard deviations $\hat{\sigma}_\omega(n)$ (square), bias $\hat{b}_\omega(q, n)$ (diamond), and MSE $\hat{J}_\omega(q, n)$ (line) as function of window length for the time point qT_s

If the system frequency is ramping (for example 10Hz/sec), with the increase of window length the bias will increase. As shown in the Figure 3, MSE is domi-

nated by stochastic error for small windows and by bias for large windows. The optimal window length (24 samples) is clearly the one where the bias and stochastic error are in balance. It should be noted that for windows larger then 24 the estimated confidence intervals do not have common points. The idea of the ICI method that determines the balance point without need for bias estimate is deduced from Figure 3 [5,6]:

The optimal window length n^ for the time instant qT_s is the one for which the set $\bigcap_{n \leq n^*} \hat{D}(q, n)$ is non-empty.*

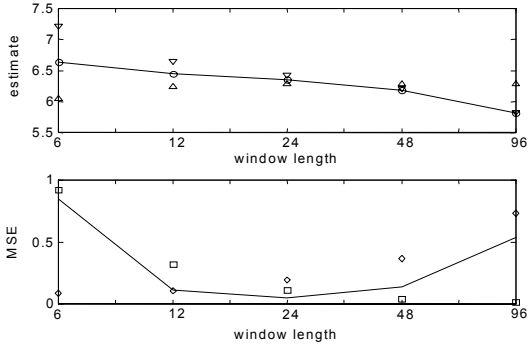


Figure 3: The ramping frequency case: Estimates of $\hat{\omega}(q)/2\pi$ (circles), common points of confidence intervals $\hat{D}_\omega(q, n)/2\pi$ (triangles), standard deviations $\hat{\sigma}_\omega(n)$ (square), bias $\hat{b}_w(q, n)$ (diamond), and MSE $\hat{J}_\omega(q, n)$ (line) as function of window length for the time point qT_s

2.5 High Precision Estimation

It is clear that we can apply the same least square method as in (6) and (7) for left-sided window, on central and right-sided windows. The expressions obtained are in the same filter form as in (8), (9), and (10), but with different formulas for calculating weight sequence, bias and standard deviation. The optimal window selection strategy, described in the section 2.4, is applied independently for each window type. To improve the final estimate these three estimates for left-sided, central and right-sided windows could be combined in the following way:

$$\hat{x}(q) = \frac{w_l \hat{x}_l(q) + w_c \hat{x}_c(q) + w_r \hat{x}_r(q)}{w_l + w_c + w_r}, \quad (21)$$

where $\hat{x}(q)$ - the final estimate of RMS, angle or frequency,
 $\hat{x}_l(q), \hat{x}_c(q), \hat{x}_r(q)$ - estimates for left-, central and right-sided windows, and
 $w_l = 1/\hat{\sigma}_l^2, w_c = 1/\hat{\sigma}_c^2, w_r = 1/\hat{\sigma}_r^2$ are weights that are corresponding to estimates of standard deviations for left-, central and right-sided windows.

3 EXAMPLES AND DISCUSSION

3.1 Step Change Simulation

Voltage drop shown in Figure 4 can occur in power systems due to faults and switching operations. The three-phase voltage signals in Figure 4 are corrupted with normally distributed noise with zero mean and standard deviation equal to 1%. Additionally, signals are distorted with 5% 2nd harmonic and 2% 5th harmonic. Bottom half of the Figure 4 shows the true RMS value and noisy estimate using the expression (4).

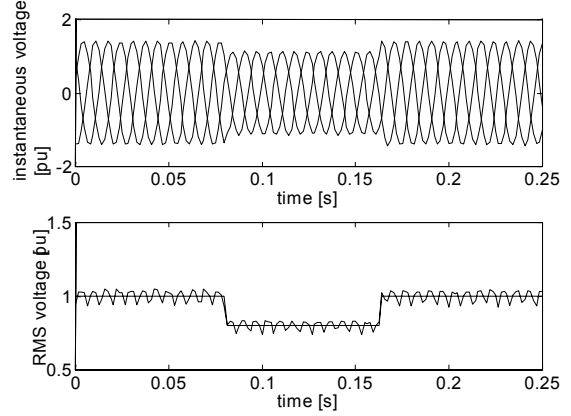


Figure 4: Three-phase signals corrupted with noise and harmonics during voltage drop conditions; true RMS and noisy estimate using the expression (4)

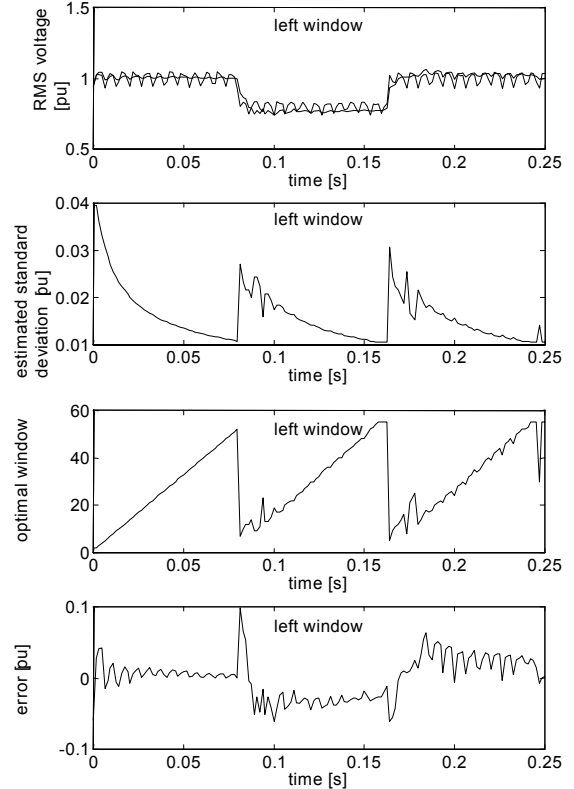


Figure 5: RMS voltage estimation using left-sided window; uppermost box compares noisy estimate using (4) and smooth estimate using nonparametric approximation (8)

The sampling frequency of the voltage drop simulation and the estimation algorithm is 640Hz. Continuous set of windows with the increment 1 was used. The maximum window length was 55 samples. In the ICI window length selection algorithm the confidence interval threshold $\kappa=1.4$ has been used. The results of the RMS voltage estimation using left-sided window are presented in Figure 5. The estimation algorithm adapts itself by changing the window length. A small window is used at the beginning leading to a large error. As long as the voltage stays constant or slow time-varying window will enlarge with each new available sample, as demonstrated in Figure 5. The outcome is the improvement of filtering and reduction of estimation error. At the instant of time when the voltage steps down, the algorithm automatically selects shorter window to track this sudden change. Now the filtering performance is degraded as indicated by increase of estimated standard deviation and error in Figure 5.

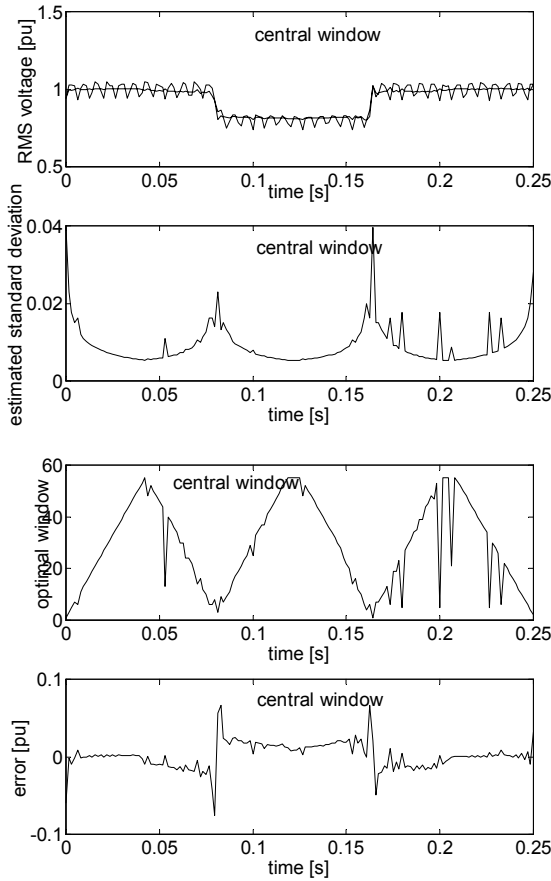


Figure 6: RMS voltage estimation using central window; uppermost box compares noisy estimate using (4) and smooth estimate using nonparametric approximation (8)

The results of estimation using the algorithm with central window and right window are presented in Figures 6 and 7 respectively. This example demonstrates how these three window types complement each other. The following three situations are present in this example:

- a) voltage is constant to the left of the estimation point and varies significantly to the right of the

point (for example the last sample before step change),

- b) voltage is constant in a large symmetric neighbourhood of the estimation point, and
- c) voltage is constant to the right of the estimation point and varies significantly to the left of the point (for example the first sample after step change).

In the case a) it is preferable to use estimate with left-sided window. By comparing Figures 5, 6 and 7, we can see that the standard deviation of this estimation is the smallest. In the final result (21) (Figure 8) this estimation enters with the largest weight. Analogously we conclude that in the case b) the central window gives the best result and the right-sided window will be the best choice for the case c). Overall performance of all three window types including combined result (21) are presented in the Table 1.

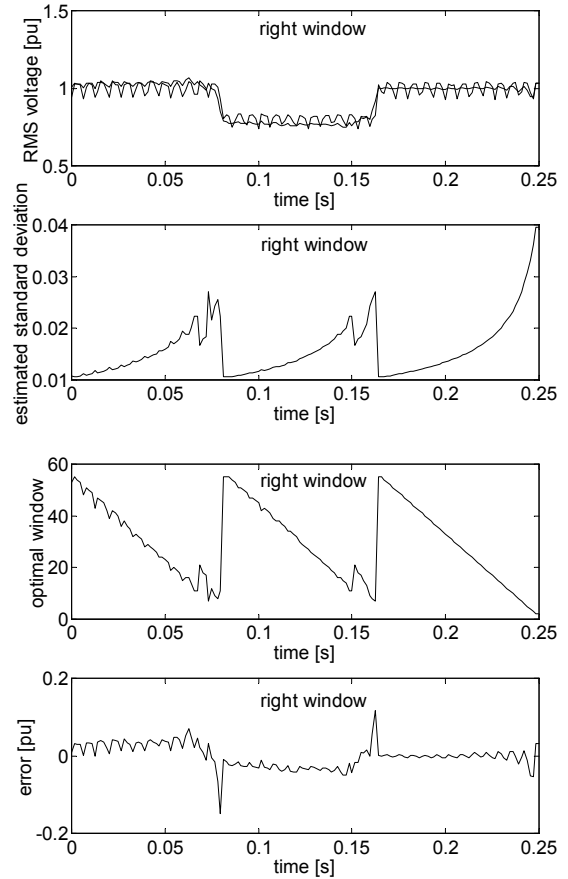


Figure 7: RMS voltage estimation using right-sided window; uppermost box compares noisy estimate using (4) and smooth estimate using nonparametric approximation (8)

| window type | maximum error [pu] | median error [pu] |
|-------------|--------------------|-------------------|
| left | 0.0979 | 0.0245 |
| central | 0.0757 | 0.0106 |
| right | 0.1502 | 0.0218 |
| combined | 0.0444 | 0.0043 |

Table 1: Performance summaries

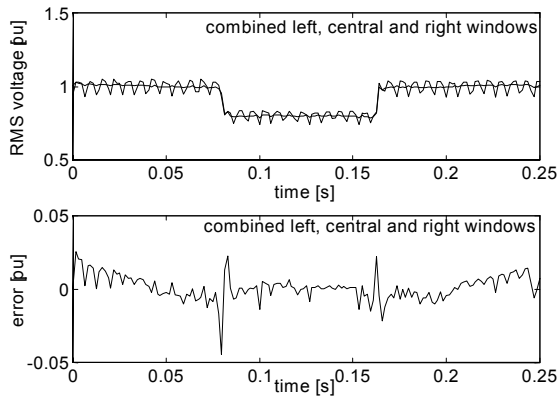


Figure 8: Final RMS voltage estimation using combination of left, central and right windows (21) compared to noisy estimate using (4)

3.2 Power Swing in ESKOM Transmission Network

The ESKOM Transmission Network is structured in such a manner that a portion of the major load centres and generator plants are remotely situated from each other. The most remote bulk load centre is the Cape Town load centre. This load centre is situated at distance of 1500 km from the pool of power stations that are generating more than 80 % of ESKOM's total electrical power. However, Cape Town is equipped with a Nuclear power station (Koeberg), which generates a total of 1800 MW at full load, and a gas fired generation plant (Acasia) with a generating capacity of 750 MW, used during peak loading conditions and emergency conditions. Figure 9 presents 400 kV lines supplying Cape Town, which are called the Cape corridor. Some of these lines are series compensated by means of series capacitor installations. Links to the pool of power plants goes through Beta and Perseus substations.

Loss of the tie through Beta in June 1996 caused the setting of large system impedance between Perseus and the generation pool. The consequence was deceleration of Koeberg rotors and a drop of frequency in the Cape corridor. As a result, Koeberg went out-of-step with the rest of the system, resulting in 4 out-of-step conditions eventually interrupted by the system separation. In this example we analyse data records obtained from DFR installed on the Bacchus-Droerivier line (Figure 9). Figure 10 presents the red phase voltage recorded on the line. Results in estimating RMS voltage during power swing using non-parametric technique for left, central, right window and combination of all three windows (21) are shown in Figure 11. These estimates are compared with noisy estimates obtained using (4). Frequency drop estimates obtained from recorded three-phase voltages using non-parametric algorithm with left, central, right and combined windows are shown in Figure 12. Adaptation of the window to frequency changes is presented in the same figure. This illustrates how the window expands for the slow-varying frequency and shrinks for sudden frequency changes.

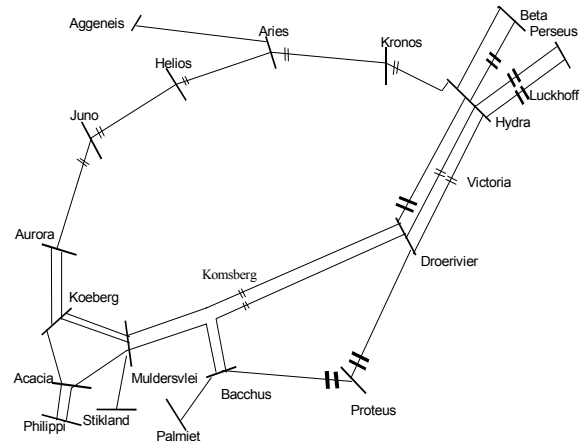


Figure 9: Southern and Western Cape Transmission System

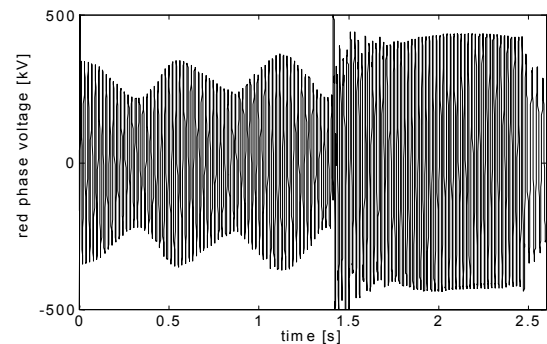


Figure 10: Red phase voltage recorded on the Bacchus-Droerivier line during the June 1996 power swing conditions

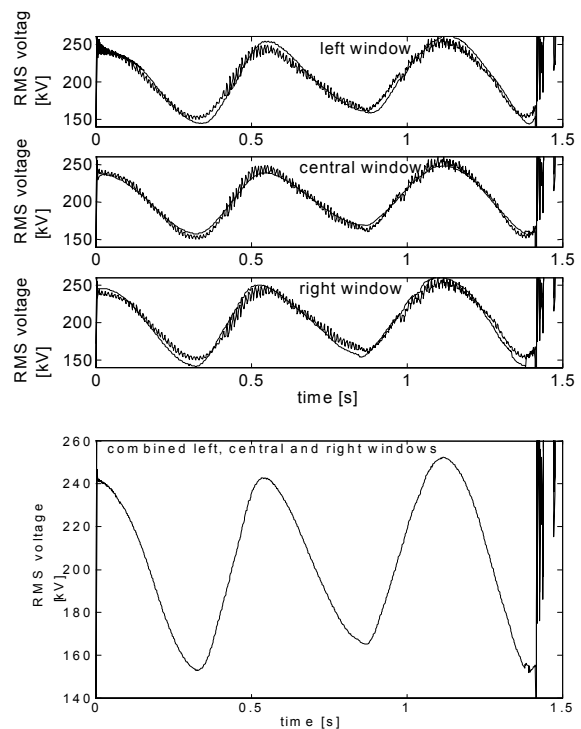


Figure 11: RMS voltage estimates according to (4) (jittery lines) and smooth estimates using (8) on the Bacchus-Droerivier line during the June 1996 power swing conditions

4 CONCLUSIONS

In this paper we have presented the local linear approximation technique for tracking phasors and frequency in power systems. This technique belongs to the class of nonparametric statistical methods where the linear model is fitted on a sliding window with variable length. The length of the window is chosen by data. For a short window, the approximation error (bias) will be small but the estimation variance could be large. On the other hand, increasing the window length could create a large bias, depending on the underlying signal change. We proposed the application of the method for automatic selection of the optimal window length that guarantees minimum error in phasor tracking and filtering in all practical situations. It has been shown that the high precision estimation is possible by combining estimates obtained using left, central and right windows. The results of testing the algorithm on simulated signals as well as recorded signals obtained from ESKOM's DFR are demonstrating clearly very good performance of the algorithm in tracking phasor and frequency variations, and in filtering harmonics and noise.

REFERENCES

- [1] IEEE Tutorial Course: "Advancements in Microprocessor based Protection and Communication; Chapter 3: Algorithms", 1997
- [2] R.Zivanovic, "Nonparametric Frequency Estimation for Power System Applications", IEEE Porto Power Tech'2001, September 2001, Porto, Portugal
- [3] J.Fan and I.Gijbels, "Local Polynomial Modelling and its Applications", Chapman and Hall, 1996
- [4] M.Akke, "Frequency Estimation by Demodulation of Two Complex Signals", IEEE Trans. on Power Delivery, Vol. 12, No. 1, January 1997, pp.157-163
- [5] Katkovnik V.Y., "On Multiple Window Local Polynomial Approximation with Varying Adaptive Bandwidths", COMPSTAT 1998, Proceedings in Computational Statistics, Physica-Verlag, pp.353-358
- [6] A.Goldenshluger and A.Nemirovski, "On spatial adaptive estimation of nonparametric regression", Math.Meth.Stat., Vol. 6, No.2, 1997, pp.135-170

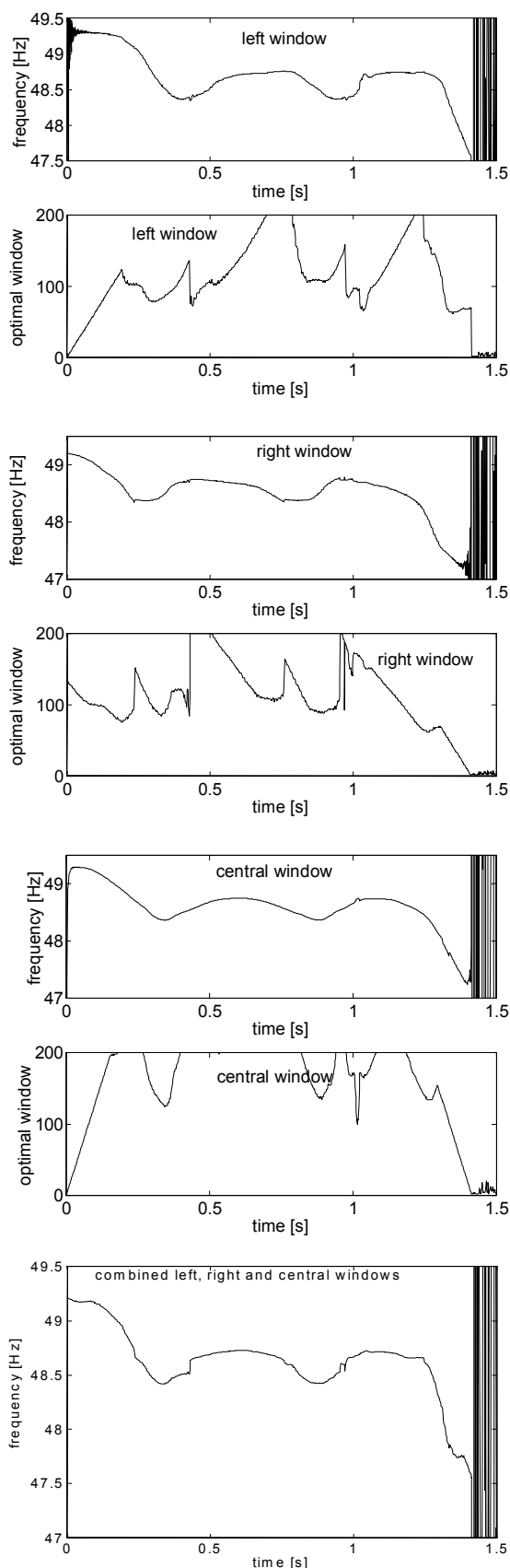


Figure 12: Frequency drop estimation and corresponding window length adaptation obtained from three-phase voltages recorded on the Bacchus-Droerivier line during the June 1996 power swing conditions